Getting Informations of Wavefunctions in Quantum Dots from the Fano Effect

Shingo KATSUMOTO, Hisashi AIKAWA, Kensuke KOBAYASHI and Yasuhiro IYE

Institute for Solid State Physics, University of Tokyo, 5-1-5 Kashiwanoha, Kashiwa, Chiba 277-8581, Japan

(Received April 30, 2004; accepted, 2004; published, 2004)

We report experimental studies of the nature of electronic wavefunctions in semiconductor quantum dots through the Fano effect. We first present clear observation of the Fano effect in an Aharonov-Bohm ring - quantum dot hybrid system. It is shown that the Fano effect can be a powerful tool to investigate the phase shifts of electrons passing over the quantum dots through the detection of electrostatic phase modulation etc. Possible existence of quantum states with anomalously strong couplings to the electrodes is discussed and experimental evidence is given by the observation of the Fano effect from the interference between ordinal transport and co-tunneling through a strongly coupled state. We also discuss that the existence of such strongly coupled states is the key to understand the long-standing problem of "in-phase Coulomb peaks" in quantum dots.

KEYWORDS: quantum dot, Fano effect, phase shift, AB effect

1. Introduction

An established view point of mesoscopic transport is to treat it as a scattering experiment[1)]. The physical quantities obtained in a scattering experiment is the forward scattering amplitude and the phase shift; The formar corresponds to the conductance (*i.e.*, transmission amplitude) and gives important information on the energy spectrum[2)]. The latter is also important to know the parity of wavefunctions and may give deterministic information on many body effects such as the Kondo effect[3)].

Phase shift can be measured *e.g.* in a Mach-Zender type interferometer geometry. A representative device to realize such a geometry in mesoscopic physics is so called Aharonov-Bohm (AB) ring, in which a quantum wire is devided into two at a furcation and then combined into one at another[4, 5)]. The first application of the AB ring method to the transport through a quantum dot was reported by Yacoby et al[6)], in which they found unnatural π-jump of the phase shift just at the Coulomb peaks. This was soon turned out to be a kind of artifact due to the two-terminal nature of the device, that is, the Osagar's reciprocity theorem imposes so called "phase rigidity" to the AB oscillation (the magnetoresistance should be an even function of the magnetic field)[7)]. In other words, the character of an AB ring as a resonator strongly appears in two-terminal conductance instead of that as a double-slit because of the unitarity of an electron wavefuntion amplitude[8)].

In order to avoid this problem, an experiment with multiple-terminal setup, which was designed to be close to a double-slit experiment, was performed[9)]. It was clarified in this experiment that the phase shift varies smoothly by π around Coulomb (resonant) peaks obeying the Breit-Wigner law. On the other hand, there appeared unexpected π-jumps of the phase shift at around mid points between the peaks, which phenomenon is called "π-lapse". In spite of extensive theoretical studies, there is no unified physical solution to this problem[10−13)]. Hence further experiment on this problem is needed.

We have presented the first clear experiment on the Fano effect[14)] in the transport through a quantum dot embedded in an AB ring[15)]. In the two-terminal setup, it has been shown there is almost one-to-one correspondence between the Fano parameter and the AB phase[16)]. This means that we can project the problem in the AB phase into that in the Fano parameter and that the Fano effect can be a tool to investigate the phase problems.

In this article we first emphasize the Fano effect as an alternative measure of the phase shift other than the AB effect. Then an essential advantage of the Fano effect – availability in a single quantum dot sturcture – is shown. This is due to the existence of quantum states with anomalously strong couplings (strongly coupled states, SCSs) to the electrodes. And it is clarified that the existence of the SCSs is the origin of "in-phase Coulomb peak" phenomenon, which is a part of the phase-lapse problem. Then we present and analyze the response of the SCSs to the magnetic field.

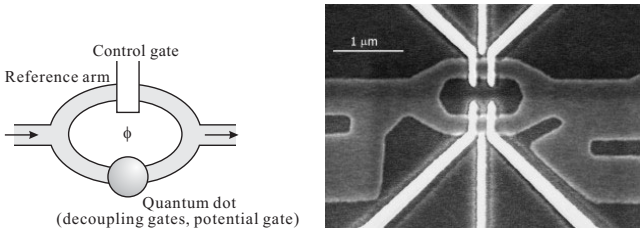

Fig. 1: Left: Schematice view of a sample. Right: Scanning electron micrograph of the sample. White regions indicate wrap-gates made of Au-Ti. Only one of the three upper gates are used to control the conductance of the reference arm.

2. Experiment

We adopt so-called wrap gate structure to define quantum dots and wires in two-dimensional electron gas (2DEG) formed in a GaAs/AlGaAs heterostructure (sheet carrier density $3.8 \times 10^{15}\ \mathrm{m}^{-2}$; mobility, $80\ \mathrm{m}^2/\mathrm{Vs}$). Quantum wire circuits are defined by using electron beam lithography and wet etching. The fine patterns of the metallic gates fabricated on the circuits form tunneling barriers, which define the quantum dots and control the parameters.

A schematic and a scanning electron micrograph of a sample are shown in Fig.1. In the sample we prepare three gates for each arm in the AB ring, two of which are used to define a quantum dot in the lower arm, and one place in the middle is used to control the electrostatic potential of the dot. In the present experiments, we do not define a quantum dot in the upper arm and only one of the three on the upper arm is used to control the conductance of the upper arm, *i.e.*, we use this arm as a "reference arm".

The samples are cooled in a dilution refrigerator down to 30 mK. The conductance is measured by a standard lock-in technique in the two-terminal setup.

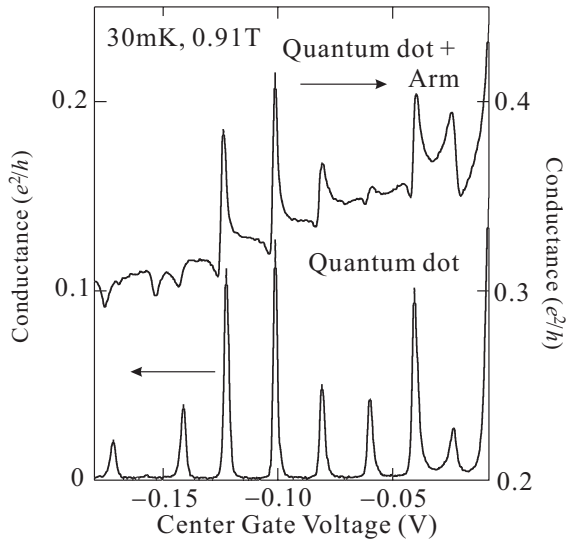

Fig. 2: Conductance of the sample as a function of the center gate voltage (V_g) with (upper curve) and without (lower curve) the conduction of the reference arm.

3. Fano effect in AB-ring - quantum dot hybrids

Figure 2 shows the low-temperature conductance of the sample as a function of the center gate voltage of the quantum dot ($V_{\rm g}$) with and without the conduction of the reference arm. When the reference arm is completely pinched off, the sample exhibits an ordinal Coulomb oscillation as shown in the lower curve in Fig.2. With opening the reference arm, the baseline of the oscillation is enhanced due to the parallel conduction and at the same time the line shapes of the Coulomb peaks are largely distorted.

The distorted line shape can be well fitted by the Fano formula described as[14)]

$$G(V_{\rm g}) \propto \frac{(\epsilon+q)^2}{\epsilon^2+1} \qquad (1)$$

where $\epsilon = \alpha(V_{\rm g}-V_{\rm res})/(\Gamma/2)$, α is a conversion factor, $V_{\rm res}$, the peak position, Γ, the width of resonance, and q, Fano's asymmetric parameter.

The Fano effect originates from the interference between a localized state and the continuum. In the present case, the conduction of the reference arm corresponds to the continuum and the states in the dot corresponds to the localized states. Hence the sign of the interference can be modified by the AB flux ϕ piercing the ring. The AB phase is in the first order $2\pi\phi/\phi_0$ where $\phi_0 \equiv h/e$ thus the change of magnetic field corresponding to $\phi_0/2$ inverts the sign of interference.

Figure 3 shows change in the Fano lineshape by that in the applied magnetic field. An inversion of the direction of the distortion by the flux change $\phi_0/2$ is clearly observed corresponding to the phase change of π. In (1), the change in the direction of distortion corresponds to that in the sign of q, which can be easily seen from that the Fano's zero (*i.e.*, the point of $G(V_{\rm g})=0$, hence $\epsilon = q$) changes its position from one side of the peak to another with the change in the sign of q.

The above discussion gives us a way to detect the direction of the variation in the phase shift by observing the Fano

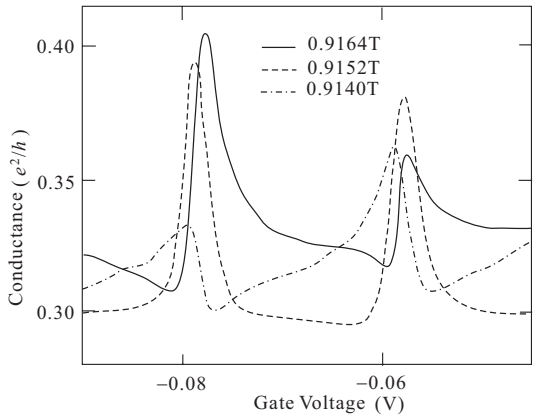

Fig. 3: Magnetic flux dependence of the Fano line shape. Change in the magnetic field between the solid line and the broken line, and also between the broken line and the dotted line corresponds to $\phi_0/4$ of the AB flux.

parameter q. In the next section we see two examples of such detections.

4. Application of the Fano effect to phase problems

4.1. Detection of electrostatic phase modulation

We first discuss application of the Fano effect to detect the phase modulation by an electrostatic potential. Here we consider the following issue: when we modify the potential of a path of electrons, this leads to a variation in the kinetic energy namely the wave vector; hence the interference term in the coherent transport should be modified through the electrostatic potential [1].

In the present experimental setup, we can utilize the control gate voltage $V_{\rm C}$ to produce such electrostatic modulation. The phase difference $\Delta\theta$ introduced by $V_{\rm C}$ is,

$$\Delta\theta(V_{\rm C}) = 2\pi(W/\lambda_{\rm F})\left(1-\sqrt{1-(V_{\rm C}/V_{\rm dep})}\right), \qquad (2)$$

where W and $V_{\rm dep}$ are the width of the gate and the pinch-off voltage of the corresponding conduction channel, respectively.

However, in the structure of an AB ring plus a control gate without quantum dot, there are many difficulties in the detection [17)]. The phase shift π by $V_{\rm C}$ indicates the increment/decrement of a single conducting channel beneath the control gate. Hence, the conductance modification caused by the channel variance is usually much larger (order of e^2/h) than that caused by the change in the interference. Furthermore, as can easily be seen in (2), $\Delta\theta$ is dependent on the channels. Thus, in conventional multichannel transport, the resultant modification of the interference is incoherent and difficult to be detected though there are a few very careful experimental reports on this subject.

By introducing a quantum dot into the structure and by having a look at the Fano effect, we can easily be free from all the above problems[16)]. The coherent transport through the dot is mainly dominated by a single conducting channel because the dot works as a filter of the wave vector, and the single channel is responsible for the Fano distortion. The variation in $V_{\rm g}$ only changes the conductance of this channel. We can safely subtract the background contribution.

[1]Note that this is different from the electrostatic AB effect

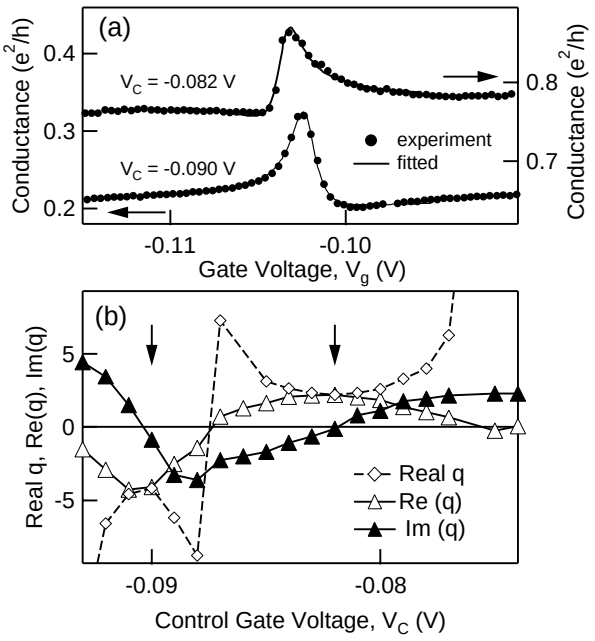

Fig. 4: (a) Transformation of Fano line shape by a change in control gate voltage on the reference arm. (b) Fitted values of real q and complex q in (1) as a function of $V_{\rm C}$.

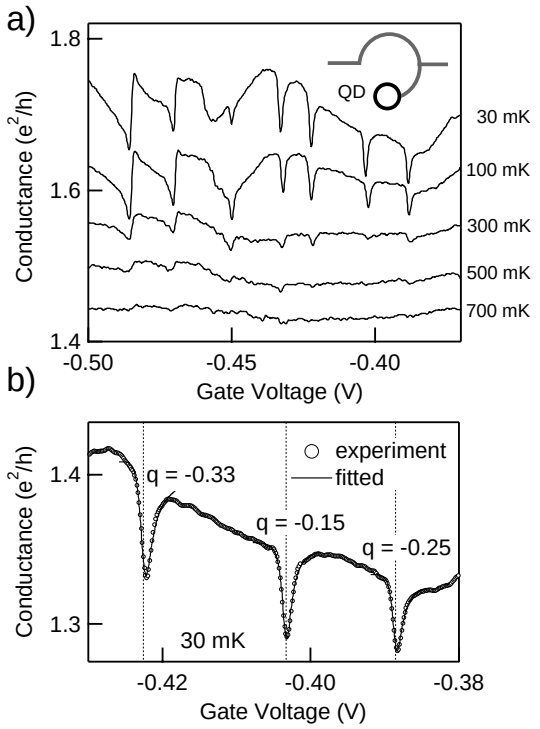

Fig. 5: (a) Temperature variation of the center gate voltage dependent conductance of a quantum wire with a side coupled quantum dot. The data are offset for clarity. (b) Example of fitting (1) to the line shapes observed in the gate-dependent conducatance.

Figure 4(a) shows the variation in line shape versus $V_{\rm g}$ with $V_{\rm C}$. A clear inversion of the direction in distortion is observed. The fitted values of real q and complex q (two components) versus $V_{\rm C}$ are shown in Fig. 4. As discussed in detail in Ref.15, replace of a real q in (1) with a complex q and taking the absolute value of resultant G is a useful technique to detect the phase-shift when the sign of real q changes[18]. Complex q follows deformed sinusoidal patterns and real q changes its sign in accordance with the real part of complex q with divergence. The clear detection of electrostatic phase modulation manifests that the Fano effect can be a powerful tool for investigating the quantum phase in the transport.

4.2. Fano effect in T-shaped connection

So far discussed is the interference phenomena in the transmission mode of the system. As discussed in the first section, in the two-terminal setup, there inevitably exists the interference between reflected waves. A simple example is the reflection at the exit of the AB ring. A portion of such interference in the reflection mode can be extracted by a cut of an end of the quantum dot. In other words, by pinching off one of the decoupling gates, we can bring the sample in Fig. 1 into such a side-coupled region (see the inset in Fig.5(a)).

Figure 5(a) shows the Coulomb oscillation of the side-coupled dot in the reflection mode, in which conductance dips appear instead of peaks. That is, the enhancement of conductance between the wire and the dot results in the enhancement of reflection at the T-shaped junction. This also appears in the temperature dependence, in that the dips themselves disappear with increasing temperature and dephasing due to thermal broadening and other decoherence factors.

Every dip reveals a clear Fano distortion as shown in Fig.5(b). In principle we can detect the direction of the phase-shift variation around a dip through the sign of real-q. We have confirmed the above by introducing small conducatance to the reference arm and by observing the AB phase.

4.3. AB ring as a resonator

If we treat the dot as a Breit-Wigner type scatterer and only consider the interference of the first order transmission wave, we can easily know the phase shift from the Fano parameter. However, the reflection part of the wavefunction shown in the above, brings complexity in the analysis of the Fano effect, which has the same origin as the two-terminal "phase rigidity" problem in the AB effect. This can easily be seen in the simplest one-dimensional model.

In order to express an AB ring circuit, we use two 3×3 S-matrices

$$S = \begin{pmatrix} \gamma & \sqrt{(1-\gamma^2)/2} & \sqrt{(1-\gamma^2)/2} \\ \sqrt{(1-\gamma^2)/2} & (1-\gamma)/2 & (1+\gamma)/2 \\ \sqrt{(1-\gamma^2)/2} & (1+\gamma)/2 & (1-\gamma)/2 \end{pmatrix}, \tag{3}$$

to express the two junctions, where γ is a parameter to express the degree of reflection. A quantum dot can be expressed as a seriese connection of three S-matrices:

$$\begin{pmatrix} \cos\theta & -\sin\theta \\ \sin\theta & \cos\theta \end{pmatrix}, \begin{pmatrix} 0 & e^{ix} \\ e^{ix} & 0 \end{pmatrix}, \begin{pmatrix} \cos\theta & -\sin\theta \\ \sin\theta & \cos\theta \end{pmatrix} \tag{4}$$

and the quantum wires connecting the dot and the junctions are expressed as

$$\begin{pmatrix} 0 & e^{iy} \\ e^{iy} & 0 \end{pmatrix}, \quad \text{and} \quad \begin{pmatrix} 0 & e^{iy/2} \\ e^{iy/2} & 0 \end{pmatrix}. \tag{5}$$

Here $\cos\theta$ is the reflection coefficient of the barrier at an end of the dot, x, y, $y/2$ are the lengths of the dot and the two wires respectively measured by the wavelength(/2π) of the electrons. Note that if we take the above two S-matrices as

the same, this special symmetry hides the order-breaking effect shown below.

Figure 6 shows typical results for three different values of y (*i.e.*, the sizes of the AB ring). From the simple definition in (4), the parity of the wavefunction in the dot should change alternatively. The result for $y = 3.75$ indeed shows such nature though that for $y = 3.0$ the direction of the distortion is the same for these three peaks. This is because the value of y is close to a resonant point $y = \pi$ and the effect of reflected wave is enhanced.

In real samples, the quantum coherence cannot be perfect as this simple model and this problem is less severe though we should be careful for the resonance in the AB ring. We will show a method to avoid this problem in the transport through a quantum dot and apply it to the problem of "in-phase Coulomb peaks" in the next section.

5. Nature of wavefunction in quantum dots and a solution to "in-phase peaks" problem

5.1. Strongly coupled states

In theoretical analysis of more realistic two-dimensional quantum dot models, and in level-statistic experiments[19] it has been found that real two-dimensinal laterally confined semiconductor quantum dots are mostly in the region between integrable systems and completely chaotic ones. It is known that in such regions, so called "scarred" wavefunctions appear[20, 21], in which clear enhancement of amplitude along corresponding classical trajectories is observed. Hence when some of such scars connect the inlet and outlet of the quantum dot, the conductance through the dot should be much larger than those of other states. Recent numerical simulations reveal the existence of such quantum states with anomalously strong couplings to the electrodes (strongly coupled states, SCSs)[22, 23, 24].

We now show that the parities of transport through other states with comparatively weak couplings to the electrodes (weakly coupled state, WCSs) are dominated by that of an SCS energetically closest to them. Let ψ_j^0 wavefunction of a WCS with energy E_j^0 and ψ_N that of an SCS with E_N, which is closes to E_j^0 among SCSs. Consider small perturbation potential V, which makes further distortion to the original dot. The perturbed wavefunction is written in the first order as

$$\psi_j \approx \psi_j^0 + \psi_N \frac{\langle \psi_j^0 | V | \psi_N \rangle}{E_j^0 - E_N}. \tag{6}$$

The transport over the dot through this ψ_j is determined by the product of transition matrix elements between ψ_j and wavefunctions in the electrodes. In RHS of (6), the second term can have much larger transition matrix element than the first one when the perturbation goes over a certain amount.

Because we have started from a non-special potential, it can be deduced that in a general potential, *i.e.*, a potential without high spatial symmetry, the parity of transmission wave through a WCS is dominated by an SCS energetically closest to it. This leads to the seriese of Coulomb peaks with the same direction of the phase variation ("in-phase Coulomb peaks"). We also speculate that the parity of the SCS should change alternatively because classical trajectories which connect the inlet and the outlet can be classified by the number of the bounce inside the dot.

5.2. Fano interference through multilevel transport in a dot

In order to examine the above inference, we have attempted to observe the Fano effect in a quantum dot $without$ outer reference arm. This can be achieved when the couplings to the electrodes are strong enough and the level broadning of a WCS Γ is larger than the avarage single electron energy level spacing. Under such condition, when the Fermi level of the electrodes coinsides with E_j (the energy of ψ_j in (6), in addition to the conduction through ψ_j, parallel conduction through ψ_N via co-tunneling exists. This parallel conduction creates a situation close to the original model of Fano[14], in which part of incident wave go over the scatterer without scattering. Hence the prallel conduction should result in the Fano interference[25].

In this "the Fano effect in quantum dot without outer interference circuit", we only have one resonator, *i.e.*, the quantum dot, which fact can be a great advantage that we can be free from the problem of "AB ring resonator" described in the previous section.

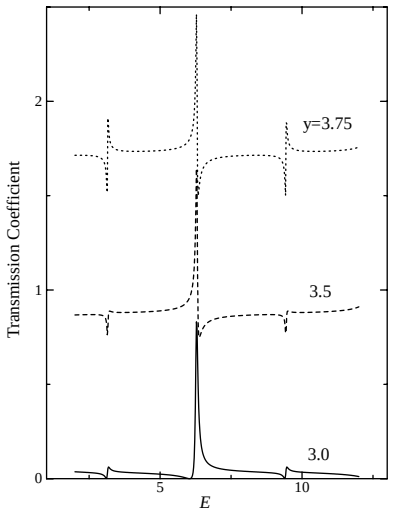

Fig. 6: Fano line-shapes calculated on the simplest one-dimensional resonator in a two-terminal AB ring geometry. $E = x$ is an effective energy and the resonance points exist at $E = \pi, 2\pi, 3\pi$. y is a parameter, which represents the spatial size of the AB ring. See the text for the detail. Other parameters, γ, θ are 0.25 and 0.2 respectively. The data are offset by 0.75.

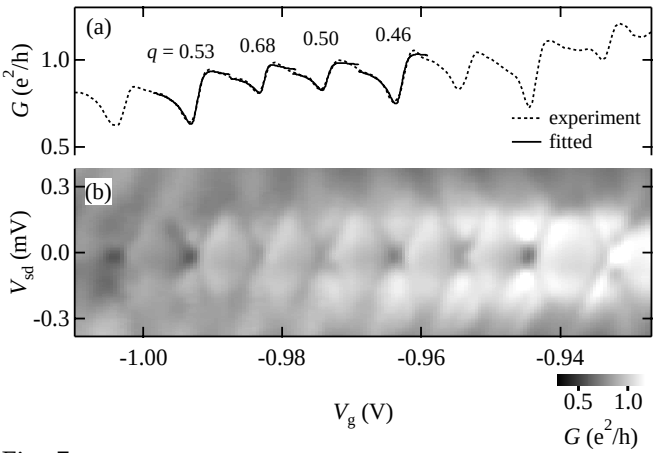

Fig. 7: (a) Coulomb oscillation (dips) in the marginal region between Coulomb blockade and open dot. (b) "Reversed" Coulomb diamonds appeared in a gray-scale plot of conductance versus source-drain voltage - gate voltage plane.

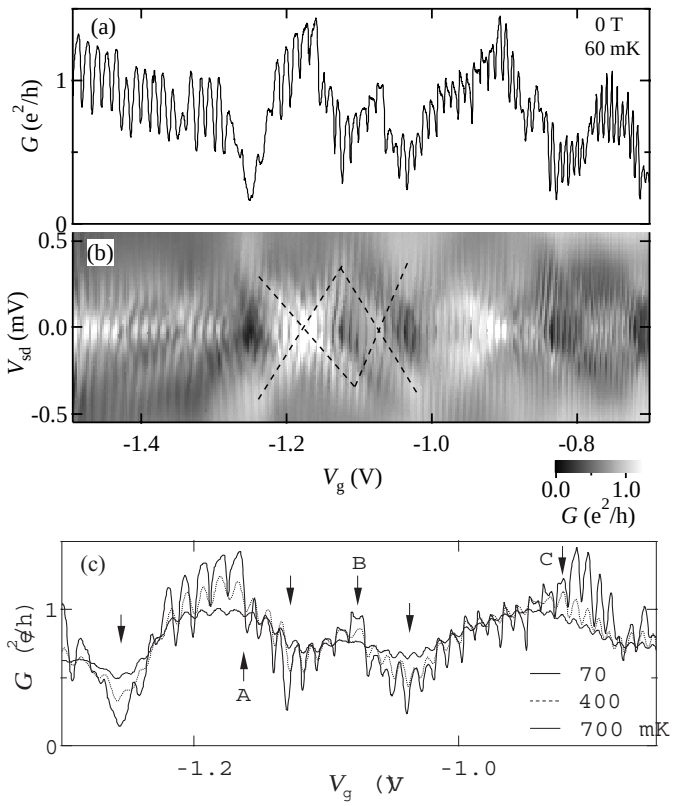

Fig. 8: (a) Coulomb oscillation in a wider range of the gate voltage. (b) Gray scal plot of the conductance in the plane of the source-drain voltage versus the gate voltage. White thin lines with slight curvature around $V_{\rm sd} = 0$ (this is due to the Fano distortion) are the reversed Coulomb diamonds. One of the overlapping diamonds is indicated by broken lines. (c) Blow up of (a). Temperature dependence is also shown. The points where the sign of the Fano parameter are indicated by arrows (A-C correspond to peaks of the background oscillation).

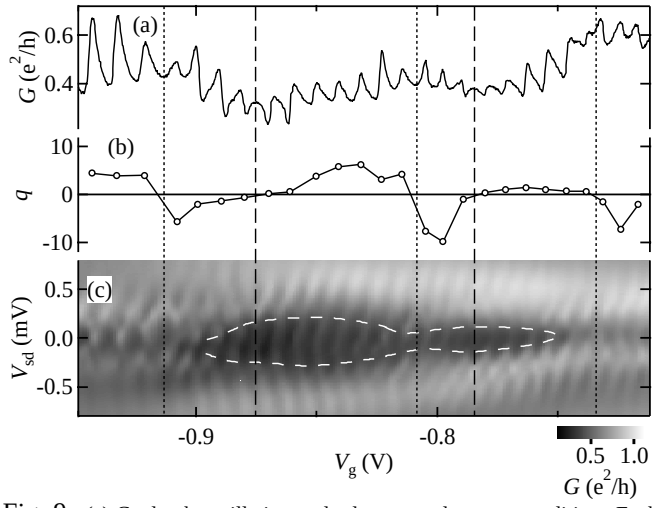

Fig. 9: (a) Coulomb oscillation under lower conductance condition. Each asymmetric line shape in (a) is fitted to obtain q as displayed in (b). Vertical broken lines indicate where the sign of q changes. (c) Gray scale plot of G versus $V_{\rm g}$ and $V_{\rm sd}$. The small Coulomb diamonds are modulated by the SCSs as presented by the white broken line.

In order to observe this effect, the reference arm is completely pinched off and the conductance through the side gates of the dot is controled to be slightly lower than e^2/h, that is the dot is in a marginal region between Coulomb blockade and open dot. Figure 7 shows Coulomb oscillation of the conductance. Though direct conduction through the dot is measured, Coulomb "dips" appear instead of peaks just like the case of side coupled quantum dot. This is due to large conduction by co-tunneling through an SCS, close to the levels corresponding to these dips. This also appears in the reversed Coulomb diamonds structures in the I-V characteristics shown in Fig.7(b). As indicated by solid curves in Fig.7(a), each dip has clear Fano distortion.

Figure 8 shows the Coulomb oscillation in a wider range of the gate voltage. The baseline of the oscillation slowly but largely oscillates, which we will call "background oscillation (BO)" henceforth. In Fig.8(b), the reversed Coulomb diamond structures show as white vertical lines with small distortion around $V_{\rm sd} = 0$, which is due to the Fano distortion. The widths of the diamonds alond $V_{\rm sd}$ are large around the valleys of the BO and small at around the peaks. As a result, in Fig.8(b), large diamond-like structures are superposed, one of which is indicated by broken lines, though they are not regular and not Coulomb origin.

The above features can naturally be explained in the model of SCS-WCS hybridization. By varying $V_{\rm g}$, the Fermi level scans resonant energy in the dot, and when it is close to a level of an SCS, the co-tunneling through it is frequent, enhancing the total conductance. Hence the background oscillation can be assigned to the co-tunneling and the change over of the SCS closest to the Fermi level. Now at around a peak of the BO, the states forming the diamonds have energy levels close to that of an SCS, thus hybridization from the SCS is severe. Because SCSs have larger spatial size due to penetration into the electrodes, the effective capacitance becomes larger at around the peaks of the BO, resulting in smaller diamonds. The conditions are opposite for the valleys of the BO and the diamonds are large.

Now the hypothesis that the "in-phase Coulomb peaks" are due to the influence of SCSs can be tested by the Fano effect in multi-level transport. In this case the Fano effect is due to the interference between the co-tunneling through ψ_N and the ordinal transport through ψ_j. The phase shift through ψ_j varies by π when the Fermi level crosses E_j resulting in the Fano distortion. When the Fermi level crosses E_N at around a peak of the BO, the phase shift through ψ_N also changes by π, which changes the sign of the Fano parameter. At around a valley of the BO, a change over of the SCS closest to the Fermi level takes place. As discussed above, the parity of the SCSs should change almost alternatively along the energy axis. The sign of the Fano parameter should hence change also at the valleys of the BO.

Figure 8(c) shows a blow up of the Coulomb oscillation in Fig.8(a) and the points where the Fano parameter changes are indicated by arrows. Apparently they are placed the peaks and valleys of the BO. Figure 9(a) shows the Coulomb oscillation at the weaker coupling conditions (the average conductance $\sim 0.5e^2/h$). The peaks show clear Fano distortion and have large enough $|q|$ for their sign to be distinguished. In Fig. 9(b), q is plotted as a function of $V_{\rm g}$ obtained by the fitting. The $V_{\rm g}$ positions where the sign of q changes are indicated by the vertical dotted and dashed lines, and they are again placed at the peaks and the valleys of the BO, respectively. In Fig. 9(c), we show a gray-scale plot of G as a function of both $V_{\rm g}$ and $V_{\rm sd}$. Though larger diamonds are not so clear as in Fig. 8(b), the modulation of widths of the small Coulomb diamonds is still

noticeable. In order to see the modulation clearer, we connect the edges of black regions that are distorted from the diamond shape due to the Fano effect with the white broken line. The vertical broken lines where the sign changes go through the narrowest points and broadest points of the region enclosed by the white line. This adds a further support to the above discussion.

At the last of this section, we would like to mention what part of the "phase lapse" issue we have clarified. The problem can be devided into two: 1) Why there appears seriese of in-phase Coulomb peaks instead of alternating parities; 2) Why there appear phase jumps between the peaks even in the four terminal setup. We believe we have answered the first question while it is difficult to give an answer to the second by our method because the Fano effect only appears around the resonant peaks.

6. Effect of Magnetic Field on SCS

When the magnetic field is applied to a quantum dot, the paths of electrons are affected by the Lorentz force, which would give significant change in the coupling strength to the electrodes. In a clean symmetric potential, this phenomenon appears as "forcusing" of electrons to the entryways resulting in characteristic magnetoresistance oscillations. When the field becomes stronger and the skewing orbits form edge states, the Landau quantization forces the outmost edge state to be the SCS. The transition between the two regions should be at around where the cycrotron diameter is the size of the dot.

Figure 10 shows a gray scale plot of the conductance of the dot under the same condition as in Fig.8 on the plane of $V_{\rm g}$ and the magnetic filed B. At low fields, aperiodic magnetoresistance oscillations are observed, which is due to the disordered forcusing of electrons. When the field is strong (above 1.5T), they change to regular oscillations. In the latter range of field, the modification of the width of Coulomb diamonds very similar to that in zero-field (Fig.8(b)) is observed and the period of the BO is exactly the same as the filling factor. The transition should take place at 1.2T from the size of the dot, which is quite reasonalbe. These observations on the response to the magentic field also supports the physical picture so far we have presented.

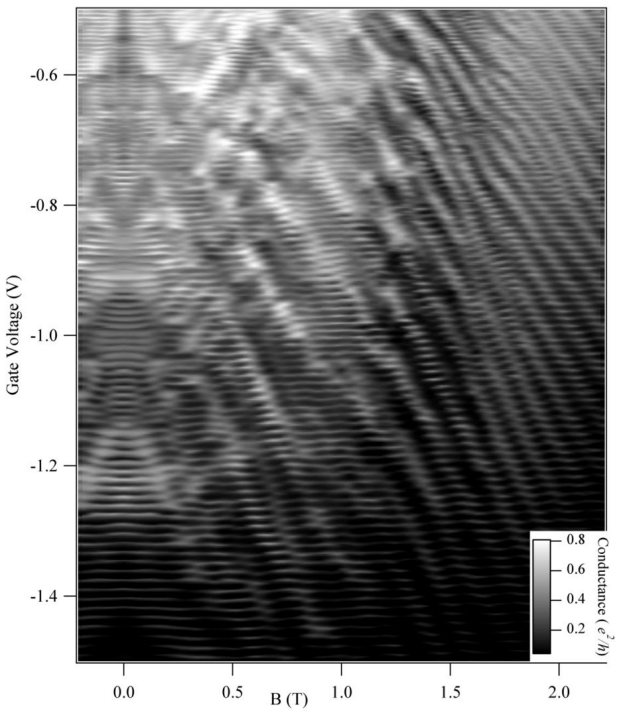

Fig. 10: Gray scale plot of the conductance of a quantum dot in the marginal region between Coulomb blockade and open dot on the plane of the gate voltage versus magnetic field.

Couclusions

We have shown that the Fano effect in the transport through quantum dots can be a powerful tool to investigate the phase problem. We have discussed that the existence of strongly coupled states can be the origin of "in-phase Coulomb peaks", to which we have given experimental evidence through the Fano effect in multi-level transport in a quantum dot without outer interference circuit. The model is also supported by the responce to the external magnetic field.

Acknowledgement

We thank A. Aharony, O. Entin-Wohlman, M. Büttiker, J. König, M. Eto, W. Hofstetter, T.-S. Kim, T. Nakanishi and T. Ando for helpful discussion.

This work is supported by a Grant-in-Aid for Scientific Research and by a Grant-in-Aid for COE Research ("Quantum Dot and Its Application") from the Ministry of Education, Culture, Sports, Science, and Technology of Japan.

1) *e.g.* see, M. Büttiker: IBM J. Res. Dev. **32** (1998) 317; Y. Imry: "Introduction to Mesoscopic Physics" (Oxford, 1997).
2) S. Tarucha, D. G. Austing, T. Honda, R. J. van der Hage and L. P. Kouwenhoven: Phys. Rev. Lett. **77** (1996) 3613.
3) J. Kondo: Solid State Physics **23** (1969) 183; D. Goldhaber-Gordon et al.: Nature **391** (1998) 156.
4) M. Büttiker, Y. Imry, and M. Ya. Azbel: Phys. Rev. A **30** (1984) 1982.
5) Y. Gefen, Y. Imry and M. Ya. Azbel: Phys. Rev. Lett. **52** (1984) 129.
6) A. Yacoby, M. Heiblum, D. Mahalu, and H. Shtrikman: Phys. Rev. Lett. **74** (1995) 4047.
7) A. L. Yeyati and M. Büttiker: Phys. Rev. B **52** (1995) 14360.
8) A. Aharony, O. Entin-Wohlman, B. I. Halperin, and Y. Imry: Phys. Rev. **B 66** (2002) 115311.
9) R. Schuster *et al.*: Nature **385** (1997) 417.
10) C. Bruder, R. Fazio, and H. Schoeller: Phys. Rev. Lett. **76** (1996) 114.
11) Y. Oreg and Y. Gefen: Phys. Rev. B **55** (1997) 13726.
12) H.-W. Lee: Phys. Rev. Lett. **82** (1999) 2358.
13) T.-S. Kim *et al.*: Phys. Rev. B **65** (2002) 245307.
14) U. Fano: Phys. Rev. **124** (1961) 1866.
15) K. Kobayashi, H. Aikawa, S. Katsumoto, and Y. Iye: Phys. Rev. Lett. **88** (2002) 256806.
16) K. Kobayashi, H. Aikawa, S. Katsumoto, and Y. Iye,: Phys. Rev. **B68** (2003) 235304.
17) S. Katsumoto, N. Sano and S. Kobayashi: J. Phys. Soc. Jpn. **61** (1992) 1153.
18) W. Hofstetter, J. König, and H. Schoeller: Phys. Rev. Lett. **87** (2001) 156803.
19) S. R. Patel, S. M. Cronenwett, D. R. Stewart, A. G. Huibers, C. M. Marcus, C. I. Duruöz, J. S. Harris, Jr., K. Campman, and A. C. Gossard: Phys. Rev. Lett. **80** (1998) 4522.
20) M. Stopa: Physica **B 249-251** (1998) 228.
21) Y.-H. Kim et al.: Phys. Rev. **B 65** (2002) 165317.
22) P. G. Silvestrov and Y. Imry: Phys. Rev. Lett. **85** (2000) 2565.
23) A. Levy Yeyati and M. Büttiker: Phys. Rev. **B62** (2000) 7307.
24) T. Nakanishi, K. Terakura, and T. Ando: Phys. Rev. **B 69** (2004) 115307.
25) J. Göres *et al.*: Phys. Rev. **B62** (2000) 2188.